Erratum: Anyon braiding on a fractal lattice with a local Hamiltonian [Phys. Rev. A 105, L021302 (2022)]

Sourav Manna, Callum W. Duncan, Carrie A. Weidner, Jacob F. Sherson, and Anne E. B. Nielsen

(Received 15 January 2023; published 2 June 2023)

DOI: 10.1103/PhysRevA.107.069901

The original paper contains an error in the interpretation of the calculated statistical phase for both the Sierpinski carpet and square lattice with 64 sites. This error was the result of an inconsistent calculation of the Aharonov-Bohm phase, which we describe in detail below. Here, we consider larger finite patches of the Sierpinski carpet and square lattice in an attempt to overcome this error, but the system sizes that we can reach with our exact diagonalization approach are not large enough to obtain conclusive results. For the Sierpinski carpet, however, the computations on the larger lattices show that the particles in the ground state preferentially localize to domains that are locally similar to a two-dimensional square lattice. This seems incompatible with the uniform density of the bulk of fractional quantum Hall states and suggests that the local model we consider on the Sierpinski carpet may not be topological. Our computations provide guidance for future searches for topology in small lattices. This topic is of great, current relevance given the recent experimental progress in the area [1].

64-site lattices. When calculating the statistical phase in the original paper we perform two main steps. First, we place two pinning potentials in the central portion of the lattice and calculate the phase gained by the state when the potentials are swapped adiabatically. Second, we find the Aharonov-Bohm phase by placing one of the potentials outside the loop while performing the loop of the swap with the other. The statistical phase, obtained as the difference between these two phases, is expected to be $1/2$ in units of π if the potentials trap one quasihole each with charge $1/2$ and the quasiholes are sufficiently separated throughout the trajectory.

In the computations performed in the original paper, we chose to place the static potential considered in the Aharonov-Bohm calculation to the corner of the lattice, in order to increase the distance between the static and moving potentials. It has come to the attention of the authors, however, that placing a pinning potential in the corner of the 64-site square or Sierpinski carpet only leads to a small amount of charge being trapped there. This is due to the ground state of the Hamiltonian without potentials and M particles having no significant particle density in the corner site. This means that even though a large pinning potential is used, there will be almost no density there to be impacted by the potential. The distribution of the charge with the corner pinning potential is shown in Fig. 1. Due to this, the calculation in the original paper does not provide the Aharonov-Bohm phase for an anyon with charge $1/2$, and the computed phases are hence not the statistical phases. From the results obtained in the original paper, it is hence not clear whether the considered models are topological or not.

Square lattice. We first discuss the model on the square lattice further. Due to the low particle density at the corners and along the edges of the lattice, one needs to put the potentials closer to the center of the lattice to trap sufficiently large charges, but this does not provide sufficient space for separated anyons on the 8×8 lattice. We have therefore further developed our exact diagonalization code to be able to consider larger lattices for the same number of particles. The larger lattice also provides further flexibility to make variations to test the robustness of the results.

Specifically, we consider a 12×12 lattice. While this is approximately doubling the number of sites, for the $M = 4$ Hamiltonian this increases the Hilbert space dimension from 6.4×10^5 to 1.7×10^7. The low particle density at the corners and edges of the lattice is seen in Fig. 2(a). We here choose a path for the exchange of the potentials that encloses no area [see Fig. 2(b)], as this eliminates the need to compute the Aharonov-Bohm phase. This was not possible in the 64-site lattice due to limited space in the bulk. We consider two variations: (i) The potentials move from one site l to the next l' following Eq. (8) in the original paper and we refer to this as narrow potentials. (ii) We do the same as (i), except that we put additional potentials of strength $V(1-\gamma)/K_l$ on K_l sites surrounding site l and additional potentials of strength $V\gamma/K_{l'}$ on $K_{l'}$ sites surrounding site l' and we refer to this as broad potentials. We take the K_l (or $K_{l'}$) sites to be the two neighbors along the path. If site l (or l') is one of the four sites at which the (green) path segments end [see Fig. 2(b)], the K_l (or $K_{l'}$) sites are instead the four nearest neighbors on the lattice. If an additional potential is applied to a site on which a potential is already applied, the potentials add.

To judge whether the potentials produce local density variations of $1/2$, we plot $\rho(z_i)$ [see Eq. (5) in the original paper] for several points along the path for the case of broad potentials and $V = 5$ in Figs. 2(b)–2(d). A video of $\rho(z_i)$ for the full exchange is given in the Supplemental Material [2]. Although density variations are mainly seen close to the potentials, there are also

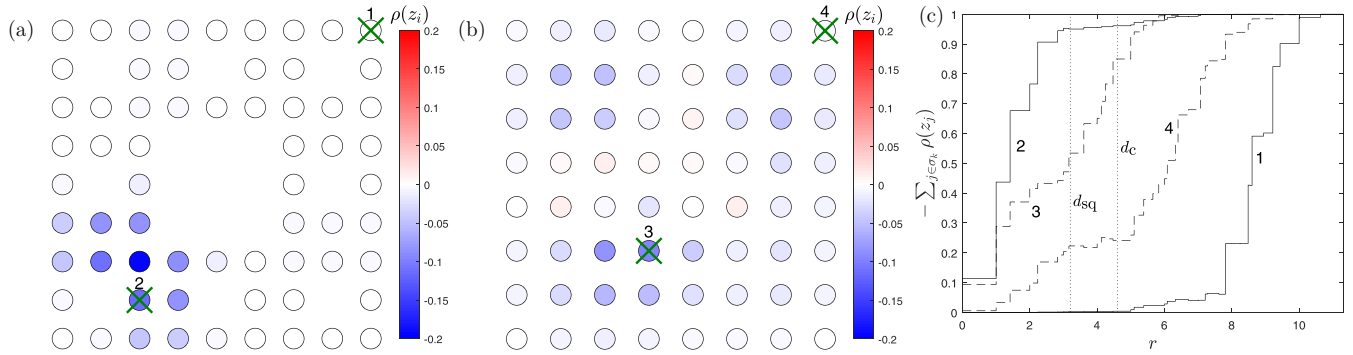

FIG. 1. We plot $\rho(z_i) = \langle n_i\rangle_{H+H_V,M-1} - \langle n_i\rangle_{H,M}$ [see Eq. (5) of the original paper] for (a) the carpet and (b) the square lattice. Here, $M = 4$ and potentials with strength 100 are placed on the two sites marked by green crosses. For the carpet, almost all the charge accumulates in the vicinity of one potential. For the square lattice, the charge is more spread out, but again there is more charge close to one potential than to the other. (c) To quantify this further, we plot the total charge $-\sum_{j\in\sigma_k}\rho(z_j)$ within a circular region with radius r and center at one of the sites on which a potential is applied. Specifically, σ_k is the set of all j for which $|z_j - w_k| \leqslant r$, and w_k is the position of the site labeled $k \in \{1, 2, 3, 4\}$ in either (a) or (b). The vertical dotted lines show half the distance between the two sites on which the potentials are applied for the square lattice (d_{sq}) and the carpet (d_{c}). If the potentials had trapped two well-separated anyons of charge $1/2$, the curves in (c) would have had plateaus at 0.5 for r large compared to the size of the anyons and short compared to the distance between the potentials. One should, however, be cautious in interpreting (c) for small lattices, as the trapped charges could have shapes far from circular. Nevertheless, considering (a) and (c) together shows that the potentials do not trap two well-separated anyons on the 64-site carpet with three particles, and (b) and (c) suggest that separated anyons are also not trapped on the 64-site square lattice with three particles. As a result, the phase computed in the paper cannot be interpreted as the Aharonov-Bohm phase obtained by moving one anyon of charge $1/2$ around the considered path.

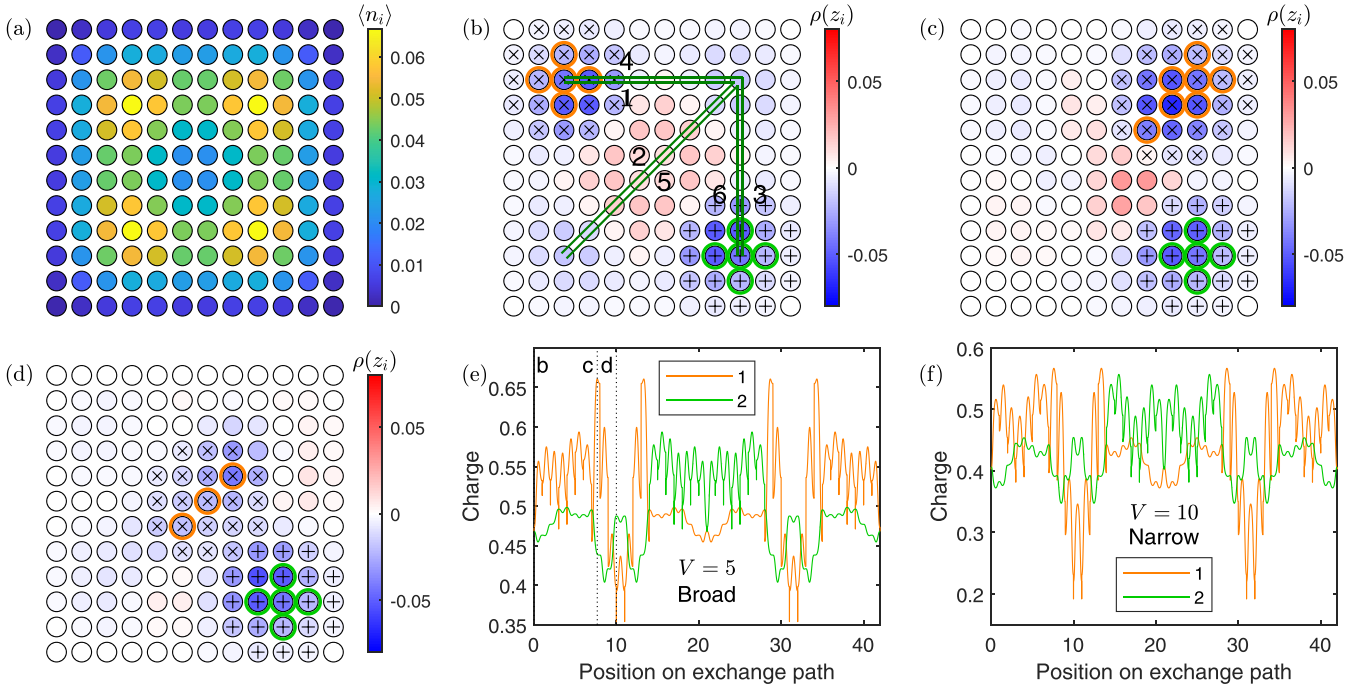

FIG. 2. (a) Particle density $\langle n_i\rangle$ of the ground state of the Hamiltonian in Eq. (1) of the original paper without potentials, $U/J \to \infty$, and four particles on a 12×12 square lattice. (b) We exchange potentials along the green paths. To begin with, potentials are placed on the sites (3,10) and (10,3). Potential 1 first moves along path 1 and then path 2, while potential 2 is fixed. Potential 2 then moves along path 3 and 4, while potential 1 is fixed. Finally, potential 1 moves along path 5 and 6, while potential 2 is fixed. The paths are shown slightly displaced to make clear that the exchange happens counterclockwise. Altogether, the path involves moving a potential from one site to the neighboring site 42 times, and for each such move we use 100 steps. We hence define the position on the exchange path as a parameter within [0,42] with two decimals. (b)–(d) show $\rho(z_i) = \langle n_i\rangle_{H+H_V,M-1} - \langle n_i\rangle_{H,M}$ [see Eq. (5) of the original paper] for different positions on the exchange path for the case of broad potentials and $V = 5$. Sites on which potentials are applied are marked with an additional green or orange ring. The local regions defined in the text are marked by crosses (region 1) and pluses (region 2). (e) shows the charge within the local regions 1 (orange) and 2 (green), i.e., the sum of minus $\rho(z_i)$ over the sites in the region, for broad potentials and $V = 5$. (f) shows the same but for narrow potentials and $V = 10$.

TABLE I. The ground-state wave function acquires the phase $\exp(i\pi\theta_s)$, when the potentials are adiabatically exchanged as in Fig. 2(b). The table gives θ_s for different strengths V and different shapes (narrow or broad, see the main text) of the potentials. The number of steps used when discretizing the path is large enough to ensure convergence of θ_s.

V	Potentials	θ_s
5	Narrow	−0.08
10	Narrow	0.03
12	Narrow	0.05
5	Broad	0.32
8	Broad	0.54
10	Broad	0.63

smaller variations quite far from the potentials. To quantify the charge, we show the sum of minus $\rho(z_i)$ over local regions around the potentials in Fig. 2(e). The local regions are selected as all sites that are at most $7/(2\sqrt{2})$ lattice spacings away from one of the sites at which a potential is applied for the case of narrow potentials. This ensures that the two local regions [marked by crosses and pluses, respectively, in Figs. 2(b)–2(d)] do not overlap. The charges are seen to often deviate by more than 10% of the ideal value. The most problematic parts are those for which one of the potentials cross the central part of the lattice. This is due to the lower density at the center of the lattice seen in Fig. 2(a). Again, however, one should be cautious about interpreting the charges in Fig. 2(e), as the shapes of the trapped charges may not fit the chosen local regions. It is more reliable to judge the presence or absence of topology based on the value and robustness of the phase acquired by the wave function for different variations of the exchange. We have computed the phase for different choices of the potentials in Table I. Some of the results are close to zero, while others are close to one half in units of π. Comparing the charges obtained for the broad potential and $V = 5$ in Fig. 2(e) to the charge obtained for the narrow potential and $V = 10$ in Fig. 2(f), it is also not clear which one is closest to the ideal case for the topological system, although the former might look slightly better as the average of the charges over the path is closer to one half. For the system sizes that we can reach with our exact diagonalization code, hence we cannot conclude whether the system is topological or not.

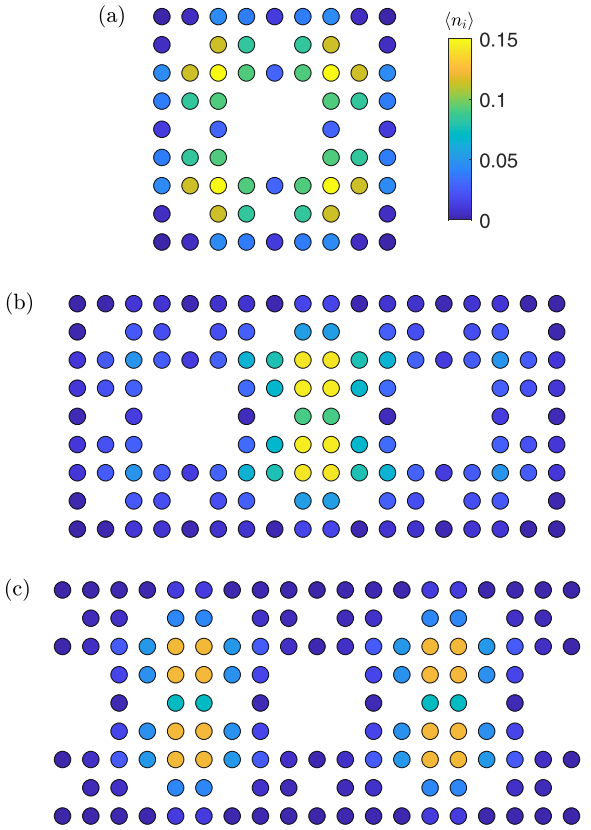

FIG. 3. Particle density $\langle n_i \rangle$ for the ground state of the Hamiltonian in Eq. (1) of the original paper without potentials, $U/J \to \infty$, and four particles for different patches of a high generation Sierpinski carpet with (a) 64 sites, (b) 128 sites, and (c) 130 sites. The highest densities are found in regions that locally look like the two-dimensional square lattice. This conclusion also holds for $M = 2$ and $M = 3$.

Sierpinski carpet. The issues with the low density in the central portion of the square lattice will of course not occur for the Sierpinski carpet, as it has no central bulk. This poses another issue—how can one generate a braiding path and consistently negate the Aharonov-Bohm phase of that path? We find that this cannot be done for any size for which we can realistically calculate the states across the braiding path. This is due to the particle density of the ground state of the $M = 4$ local Hamiltonian, which we show for various patches of the Sierpinski carpet of varying size in Fig. 3. We find that contrary to the 64-site lattice of the original paper, on larger patches the ground state has high density along quasi-two-dimensional domains that form between patches of the original 64-site lattice. To calculate the statistical phase, paths need to be constructed by moving between multiple quasi-two-dimensional regions (with the local coordination number being four) of sufficient size to support two quasiparticles with no overlap, which requires lattices beyond the size capable with the methods implemented here. We note, however, that the very nonuniform density on the patches of the carpet seems inconsistent with the uniform densities observed for the bulk of fractional quantum Hall states on two-dimensional lattices. This gives a hint that the model on the Sierpinski carpet may not be topological.

Conclusions. We have shown that the phases given in Table I of the original paper cannot be interpreted as statistical phases, and as a consequence the results of the original paper do not show whether the systems are topological or not. We have here tried to remedy this by considering larger lattices. Considering exchanges on a 12×12 square lattice, different variations led to phases that differed by more than one half in units of π. To judge whether the model is topological or not on a square lattice, even larger system sizes are needed, which are beyond the exact diagonalization methods utilized, or alternatively one could try to optimize the chosen potentials [3]. For larger patches of the Sierpinski carpet, we find that the particle density tends to accumulate at regions of the lattice that locally look similar to a two-dimensional square lattice. As fractional quantum Hall states tend to have uniform densities in the bulk, this might suggest that the states on the carpet are not topological.

We have shown that for future explorations of the construction of other local Hamiltonians that could support topological quasiparticles, it is critical that one should aim for ground states with high particle densities across a large connected region of the lattice. This will make the construction of consistent paths to calculate the statistical phase simpler. Future research on which local properties of a Hamiltonian can most impact the extent of quasiparticles and allow for their generation across large regions of two-dimensional lattices, perhaps in combination with the optimization of the trapping potentials, would be fruitful.

The authors thank Blazej Jaworowski for bringing the error in the original paper to their attention.

---

[1] J. Léonard, S. Kim, J. Kwan, P. Segura, F. Grusdt, C. Repellin, N. Goldman, and M. Greiner, Realization of a fractional quantum Hall state with ultracold atoms, arXiv:2210.10919.

[2] See Supplemental Material at http://link.aps.org/supplemental/10.1103/PhysRevA.107.069901 for a video of the time evolution of $\rho(z_i)$ during the exchange of the broad potentials with $V = 5$.

[3] N. S. Srivatsa, X. Li, and A. E. B. Nielsen, Squeezing anyons for braiding on small lattices, Phys. Rev. Res. **3**, 033044 (2021).